19e Journées de l'Hydrodynamique
26 – 28 novembre 2024, Nantes

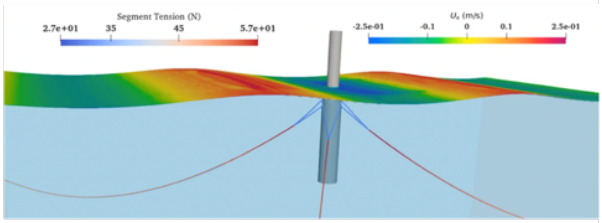

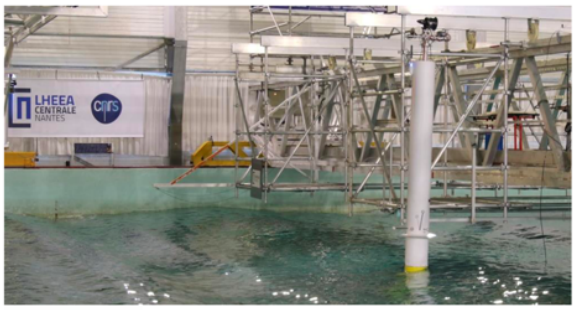

ANALYSE DES CRITÈRES DE FIN DU DÉFERLEMENT DES VAGUES

ANALYSIS OF WAVE BREAKING TERMINATION CRITERIA

J. WANG[(1)], J. HARRIS[(1)], M. YATES[(1)], S. MOHANLAL[(1,2)]
jiankai.wang@enpc.fr ; jeffrey.harris@enpc.fr ; marissa.yates@enpc.fr
s.mohanlal@hrwallingford.com

[(1)]LHSV, Ecole des Ponts, EDF R&D, Chatou, France
[(2)]Coasts & Oceans, HR Wallingford, Wallingford, Oxfordshire, UK

Résumé

Le rapport entre la vitesse horizontale des particules à la crête et la célérité de la vague, noté B, ainsi que le *nombre de Froude relatif au creux*, noté $RTFN$, ont été proposés comme deux critères universels potentiels pour estimer le déferlement des vagues dans les modèles de propagation de vagues à phases résolues. Ces critères sont considérés comme applicables à différentes profondeurs d'eau, y compris les eaux peu profondes, intermédiaires et profondes, ainsi qu'à divers types de déferlement, tels que le déferlement glissant et le déferlement plongeant. Cependant, le critère B montre une applicabilité limitée à estimer la fin du déferlement, tandis que le critère $RTFN$ tend à sous-estimer la célérité de la vague dans le creux lorsqu'il s'agit d'estimer le début du déferlement. Par conséquent, cette étude vise à évaluer la combination des deux critères, en utilisant le critère B pour déterminer le début du déferlement et le critère $RTFN$ pour en déterminer la fin, en proposant un critère hybride, B-$RTFN$, où la valeur critique du début du déferlement est notée $B_{on} = 0.85$ et celle de la fin est $RTFN_{off} = 1.2$.

Les processus de déferlement des vagues sont analysés en utilisant une approche d'éléments de frontière complétement non-linéaire, en comparant le critère B avec le critère B-$RTFN$. Cette analyse est réalisé pour deux types de bathymétrie : une barre trapézoïdale et une pente constante. À travers l'analyse de l'enveloppe des vagues, des variations de célérité, des zones de déferlement et de la dissipation d'énergie, il est constaté que sous l'hypothèse d'eau peu profonde, le critère combiné est applicable aux déferlements glissant et plongeant, et est en bon accord avec des expériences ainsi qu'avec les résultats obtenus en utilisant le critère B. Le critère B-$RTFN$ montre une applicabilité plus générale que le critère B pour déterminer la fin du déferlement des vagues, car il ne nécessite pas de calibration pour chaque cas de test comme une valeur unique est proposée. Cependant, en eau profondeur intermédiaire ou en eau profonde, des méthodes plus précises pour calculer la célérité des vagues peuvent être nécessaires pour améliorer l'évaluation précise.

Abstract

The ratio of the horizontal particle velocity at the crest to the crest celerity, denoted as B and the *Relative Froude Trough Number*, denoted as *RTFN* have been proposed as two possible universal criteria for estimating wave breaking in phase-resolving wave propagation models. These criteria are considered applicable in different water depths, including shallow, intermediate, and deep water, as well as for various types of wave breaking, such as spilling and plunging breaking. However, the B criterion shows limited applicability in estimating the wave breaking termination, while the *RTFN* criterion depends on the trough celerity which is difficult to determine accurately. Therefore, this study aims to evaluate the combination of the two criteria, using the B criterion to determine the breaking onset and the *RTFN* criterion to determine its termination, proposing a hybrid criterion, *B-RTFN*, where the critical value of breaking onset is denoted as $B_{on} = 0.85$ and that of termination as $RTFN_{off} = 1.2$.

Wave breaking processes were analyzed using a fully nonlinear boundary element approach by comparing the B criterion with the *B-RTFN* criterion. This analysis considered two types of bathymetry: a trapezoidal bar and a constant slope. Through analysis of the wave envelop, celerity changes, breaking regions and energy dissipation, it is found that in shallow water conditions, the combined criterion is applicable to both spilling and plunging wave breaking, and in good agreement with experiments and with the results obtained using the B criterion. The *B-RTFN* criterion demonstrates more general applicability than the B criterion in determining the wave breaking termination, because it does not require calibration for each test case since a single value is proposed. However, in intermediate and deep water conditions, more accurate methods for calculating the wave celerity may be required to improve the evaluation of this criterion.

I – Introduction

A breaking criterion, which determines when and where wave breaking occurs, i.e., when the associated energy dissipation begins and ends, plays an important role in the study and modeling of wave propagation. Many wave characteristics are used to estimate the phases of wave breaking, including onset and termination. Criteria such as the front crest slope [12], vertical velocity [8], and local energy growth rate [15] are employed from geometric, kinematic, and dynamical perspectives [14]. However, most of these methods are applicable to specific water depths and types of wave breaking, e.g., spilling and plunging, requiring calibration under varying limit conditions.

In recent years, the ratio of the horizontal particle velocity at the crest to the crest celerity, denoted as $B = u_{crest}/c_{crest}$ [1], has been proposed as a universal criterion. It has been demonstrated to have broad applicability for different types of breaking waves, including spilling and plunging, as well as for various depths ranging from shallow and intermediate water to deep water [3], except for some exceptions [13]. However, while there are some semi-empirical relations for breaking dissipation, calibration is still required to accurately predict breaking termination [9].

Another criterion, the *Relative Trough Froude Number*, denoted as *RTFN*, was proposed by Utku (1999) [16], and redefined by Okamoto et al. (2006) [10]. It is defined as $RTFN = (c_{crest} - u_{trough})/c_{trough}$ and has been applied to identify wave breaking for a range of water depths. The *RTFN* criterion has been validated using experimental observations and theoretical analyses for linear waves, solitary waves, and second-order Stokes waves.

Compared to other criteria, such as the vertical velocity, front crest slope, and B criterion, it has been shown to determine the location of wave breaking termination more universally, using the same, constant threshold as for breaking termination, $RTFN_{off} = 1.2$ [11]. However, in the very shallow water, calculation of the trough celerity becomes difficult, because in the very shallow water region near the trough, wave transformation results in a very gentle free surface gradient, complicating the detection of the precise location of the trough. Additionally, wave breaking causes higher harmonics to separate from the main wave, making it even more challenging to identify the trough position associated with a given wave crest. [11].

In this study, a combined criterion, referred to as the $B - RTFN$ criterion, is implemented in a fully nonlinear boundary element method (*Numerical Wave Tank* model, denoted as NWT) [6], and compared to the results of [9] using only the B criterion. The combined criterion integrates the B-criterion to estimate breaking onset and the $RTFN$ criterion to estimate breaking termination.

II – Methodology

The NWT model is based on fully nonlinear potential flow theory, where wave propagation is modeled as an irrotational, inviscid, and incompressible flow in the two-dimensional plane (x, z). The governing equation for the velocity potential, ϕ, is given by Laplace's equation,

$$\nabla^2\phi = 0 \tag{1}$$

with the flow velocity $\mathbf{u} = \nabla\phi$ in the fluid domain Ω and on the boundary Γ. The kinematic and dynamic boundary conditions of the free surface Γ_f can be written as,

$$\frac{\partial\eta}{\partial t} = \frac{\partial\phi}{\partial z} - \frac{\partial\eta}{\partial x}\frac{\partial\phi}{\partial x} \tag{2}$$

$$\frac{\partial\phi}{\partial t} = -g\eta - \frac{1}{2}|\nabla\phi|^2 - \frac{p_a}{\rho} \tag{3}$$

where η denotes the elevation of free surface, p_a denotes the free surface pressure (normally, p_a , representing the atmosphere pressure, is set to 0), g is the gravitational acceleration, and ρ is the fluid density.

The relative absorbing surface pressure p_a [9] is applied to the Eq.(3) when wave breaking is activated, i.e., B exceeds B_{on}, and the $RTFN$ criterion determines the end of breaking when $RTFN$ decreases below the threshold $RTFN_{off}$, such that:

$$\begin{cases} \text{Breaking onset, if : } B = \dfrac{u_{crest}}{c_{crest}} \geq B_{on} \\ \text{Breaking termination, if : } RTFN = \dfrac{c_{crest} - u_{trough}}{c_{trough}} \leq RTFN_{off} \end{cases} \tag{4}$$

where u_{crest} and u_{trough} represent the free surface horizontal velocity of the particles at the crest and trough of a wave, respectively. In the definition of the $RTFN$ criterion, the trough of the wave is defined as the trough preceding the wave crest (see Fig. 1). When $B \geq B_{on}$, the energy dissipation, following the analogy with a hydraulic jump [4], is applied to the breaking zone, with (x_l, x_r) positioned near the troughs immediately preceding and following the crest, which ensures that the normal velocity of particles at the free surface, denoted as $|\frac{\partial\phi}{\partial n}|$, remains less than $\varepsilon|\frac{\partial\phi}{\partial n}|_{\max}$, where $\varepsilon \ll 1$ (specifically,

$\varepsilon = 10^{-4}$ here) [5]. Until $RTFN > RTFN_{off}$, energy dissipation is applied over this spatial extent, using a spatial smoothing function [9] to avoid abrupt changes.

During the simulation, small oscillations are observed on the free surface near the wave breaking region, which affect the precise determination of crest and trough positions. For troughs, the flat profile makes pinpointing their locations more complex. In such cases, incorrectly applied energy dissipation can exacerbate free surface oscillations, ultimately leading to simulation instability. Following [10], to simplify the calculation of the wave celerity and to enhance stability of the simulation, the Ursell number is introduced to distinguish between nonlinearity dominant and dispersion dominant regions, as follows,

$$Ur = \frac{aL^2}{d^3} \tag{5}$$

where a denotes the wave amplitude, L is the wavelength, and d represents the still water depth. In deep water, where $Ur < 40$, the wave celerity is determined as the slope of the least-squares linear fit of the position of the crest or trough node, denoted as $[x_1, x_2, ..., x_9]$ during the preceding nine time steps, denoted as $[t-8\Delta t, t-7\Delta t, ..., t]$, where t represents the actual time and Δt denotes the time step. In shallow water, where $Ur > 60$, under the assumption of nonlinear shallow water, the wave celerity is calculated analytically as follows,

$$\begin{cases} c_{crest} = \sqrt{gd} \\ c_{trough} = \sqrt{g(d+\eta)} \end{cases} \tag{6}$$

where η is the free surface position relative to the still water level. In fact, as the wave approaches the slope, the level of the shoreline changes and is no longer equivalent to the still water level. Furthermore, the wave trough exhibits a relatively gentle profile with minimal vertical variation, as will be shown in the test cases below, which is why η is considered in the trough celerity. [10].

When $Ur \in [40, 60]$, the wave celerity is calculated as a weighted average of the deep and shallow water values. It is important to note that for the B criterion, the wave celerity is calculated using only a linear fit. To distinguish between them, the single linear fit method is referred to as LF, while the aforementioned method is called the hybrid method, serving as the default approach for the B-$RTFN$ criterion.

III – Results and discussion

III – 1 Periodic waves propagating over a bar

The bathymetry of the Beji and Battjes (1993) [2] experiments, referred to as case BB (wave propagation over a bar, as illustrated in Fig. 1), is utilized to validate the $B - RTFN$ criterion. In this configuration, the constant water depth is $0.4\,m$ in the wave generation zone and leading up to the bar. A trapezoidal bar is located in the range of $x \in [10.8, 21.79]\,m$, featuring a front slope of 1/20 and a rear slope of 1/10. At the crest of the bar, the still water depth is reduced to $0.1\,m$. To prevent wave reflections, a numerical absorbing beach extends from $x = 25\,m$ to the end of the computational domain. For this case, periodic waves with a wavelength of $4.8\,m$, a wave height of $0.042\,m$ and a period of $2.5\,s$, are generated by the piston wave maker at the left side of the domain.

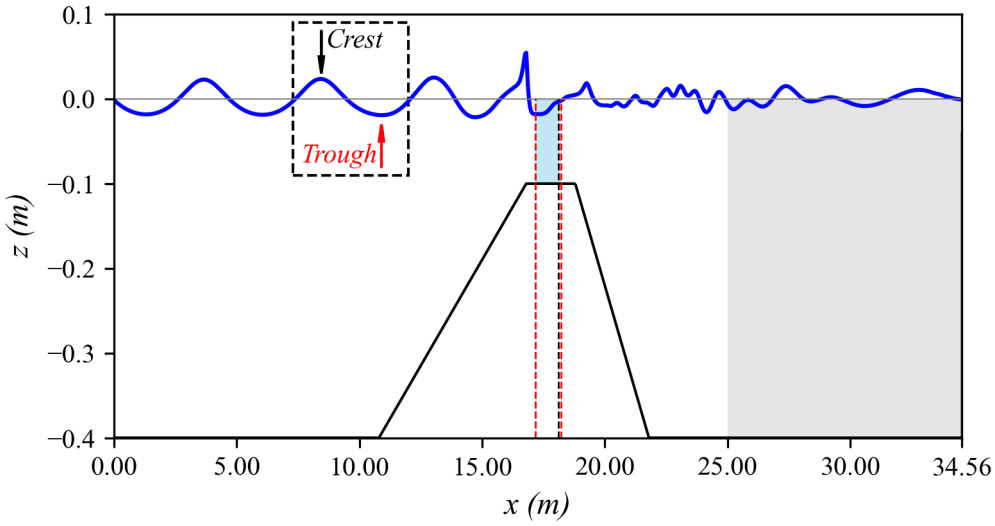

Figure 1: Bathymetry of Beji and Battjes (1993) showing the breaking region (blue) and the absorbing region (gray) applied in the numerical tests.

Regarding the BB bathymetry, the periodic waves become steeper and undergo plunging breaking as they pass over the trapezoidal bar. Fig. 2a shows the evolution of the $RTFN$ and B values. It is important to note that the particle velocity u_{trough} differs from the wave celerity by two orders of magnitude, therefore, during the discussion, the focus is primarily on analyzing the influence of the wave celerity. It is observed that the two criteria, B and $B - RTFN$, corresponding to the interval $[x_{on}, x_{off}]$, are in good agreement (for the B criterion, $x_{on} = 17.17\,m$ and $x_{off} = 18.11\,m$; for the $B - RTFN$ criterion, $x_{on} = 17.18\,m$ and $x_{off} = 18.22\,m$). As illustrated in Fig. 2a, the breaking zones for the B and B-$RTFN$ criteria are shaded in red and gray, respectively. The results indicate that the $RTFN$ value decreases sharply and falls below the threshold $RTFN_{off}$ as it approaches the end of the breaking zone. In comparison to Fig. 2b, it corresponds to a sudden increase in the trough celerity, while the crest celerity remains constant. This discrepancy arises because the trough has already traversed the shallow water region above the bar, unlike the crest that follows. Consequently, the water depth d increases, which in turn increases $c_{trough} = \sqrt{g(d+\eta)}$. Here, the influence of the water depth d is the dominant factor, although the free surface elevation η also increases slightly (see Fig. 3). In contrast, $c_{crest} = \sqrt{gd}$ remains constant, along with the corresponding water depth. Eventually, the $RTFN$ decreases sharply and wave breaking stops. It should be noted that, the x-axis is uniformly represented by the position of the wave crests x_{crest} when representing both the crest and corresponding trough celerity, even if the wave troughs always appear before the wave crests.

In Fig. 2, the wave celerity at the crest that is calculated by the linear fit (LF, dashed black line) differs from that obtained using the hybrid method (solid blue line), particularly from around $x = 14\,m$. However, the two are relatively close in the narrow region above the bar, which also explains why the onset position of wave breaking is similar for both cases.

Fig. 3 illustrates the profiles of the free surface at different moments in time, with the upper (crest) and lower (trough) envelopes represented in blue and red, respectively.

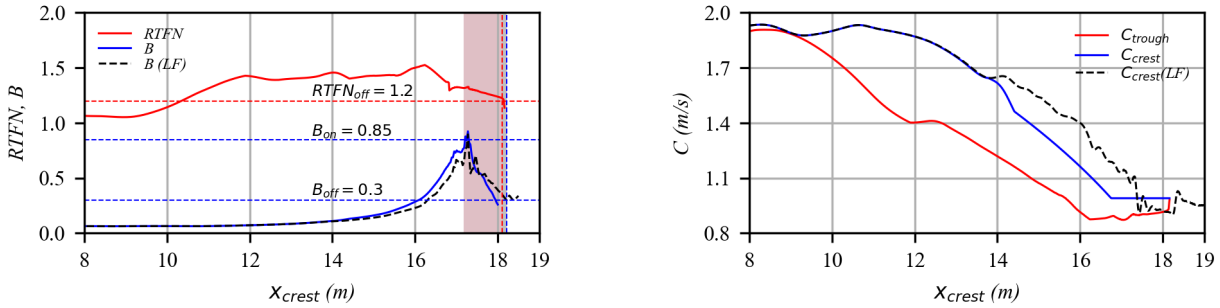

(a) Evolution of B and *RTFN* (b) Evolution of the celerity

Figure 2: Breaking region in the case of Beji and Battjes (1993)

During wave breaking, $t \in [t_{on}, t_{off}]$, the energy dissipation has a significant effect on the upper envelope position, leading to a gradual decrease in wave height. In contrast, the impact on the lower envelope position is minimal, with the elevation of the troughs showing an overall slow upward trend.

A comparison of the two criteria Fig. 3a and Fig. 3b, shows that for the *B-RTFN* criterion, the wave height decreases more during the wave breaking process. By the time the wave breaking stops, the back slope of the wave crest has become relatively gentle. However, when using the B criterion, the back slope still shows a noticeable concavity. This is related to the rate of energy dissipation. In the NWT model, the hydraulic jump analogy is used to estimate the energy dissipation of breaking waves. Mohanlal et al. (2023) [9] proposed an energy dissipation rate as a function of the celerity, expressed as $\Pi_b = b(c_{crest})^5/g$, where they assumed b is a constant related to the breaking intensity. Consequently, Π_b depends only on the wave celerity at the crest. This explains that the difference in wave height actually reflects the difference in energy dissipation, as illustrated in Fig. 7a, and the essence of the difference in energy dissipation lies in the differences in the celerity calculation.

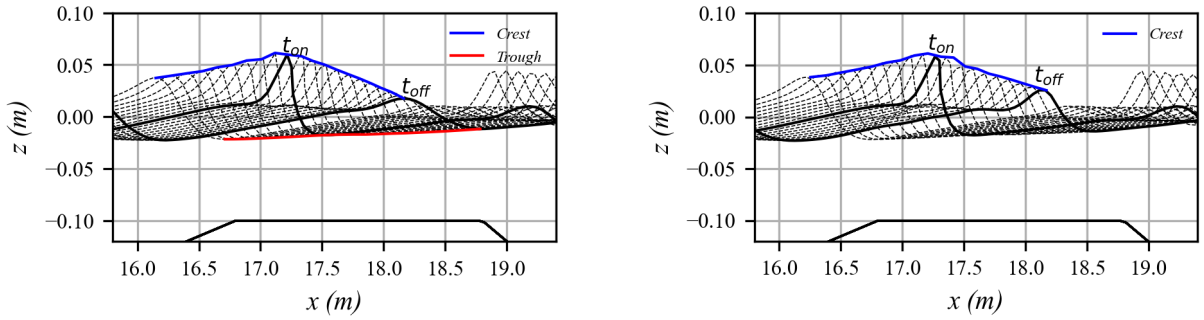

(a) using *B-RTFN* criterion (b) using B criterion

Figure 3: Envelope of the breaking wave, showing snapshots of the free surface position every 10 time steps, in the BB test case

The following section focuses on comparing the variations in the free surface elevation over time during propagation and breaking, as shown in Fig. 4. Specifically, four observation points are selected: at the middle of the front slope ($x = 15.8\,m$), at the crest of the slope ($x = 16.8\,m$), at the center of the breaking region ($x = 17.8\,m$), and at the edge of the back slope ($x = 18.8\,m$). The results indicate that both the experimental data and numerical results exhibit good agreement before and during wave breaking. However,

after that, e.g., $x = 18.8\,m$, the peak elevation when using the $B - RTFN$ criterion is lower than the experimental and B criterion results. This is because the $B - RTFN$ criterion causes greater energy dissipation than the B criterion, as calculated by $\int \Pi_b \, dt^*$, corresponding to the red shaded area shown in Fig. 7a, which leads to a reduction in the free surface elevation.

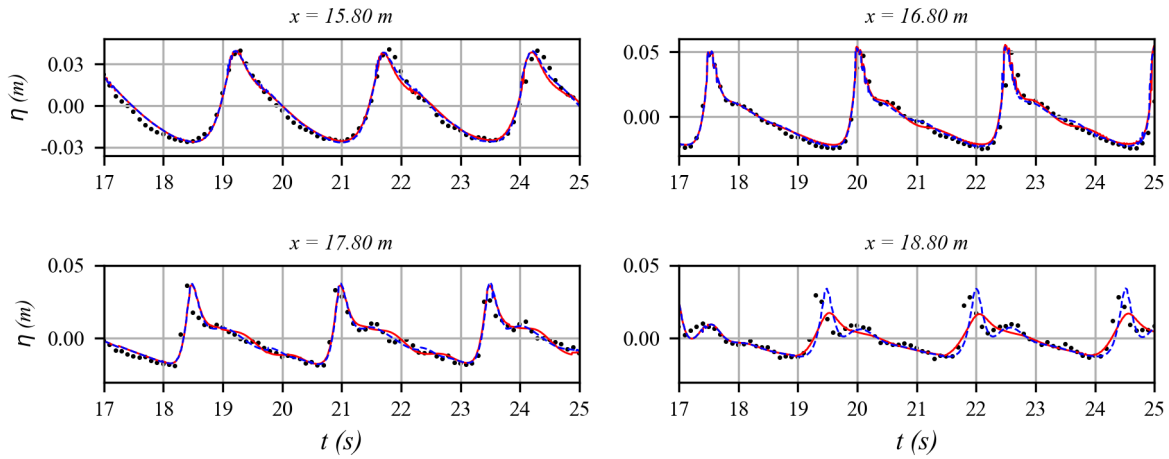

Figure 4: Temporal evolution of the free surface for the BB experiments (black dots), simulation with the $B - RTFN$ criterion (red line) and simulation with the B criterion (dashed blue line).

III – 2 Periodic waves propagating over a slope

In addition to the BB bathymetry, the *B-RTFN* criterion is applied to test cases of waves propagating over the bathymetry profile of Hansen and Svendsen (1979) [7], designated as case HS, in which waves propagate up a contant slope of 1/35 (see Fig. 5). The analysis is completed for regular, periodic waves with a wavelength of $1.43\,m$, a wave height of $0.095\,m$, and a period of $1.0\,s$. In this configuration, the still water depth in the wave generation and subsequent flat bottom zone is $d_0 = 0.36\,m$, while the minimum depth at the crest of the ramp is $d_p = 0.03408\,m$. The beginning of the slope is located at $x_p = 7.16\,m$. An absorption zone, which begins from the peak of the ramp at $x = 18.3296\,m$, is positioned at the right side of the domain.

In the experiments of HS, waves propagate over a mild slope and spilling breaking is observed starting at $x_{on} = 14.88\,m$. Since the bathymetry has a constant slope to the shoreline, wave breaking will continue until the end of the domain; therefore, the critical value of the B termination criterion, B_{off} is set to 0, while B_{on} and $RTFN_{off}$ remain unchanged. Finally, the periodic waves break at $x_{on} = 15.00\,m$ for the *B-RTFN* criterion and at $x_{on} = 15.07\,m$ for the B criterion, as shown in Fig. 6. After that, the value of *RTFN* remains relatively constant, or may even increase, as shown in Fig. 6a. In this case, the critical value $RTFN_{off}$ does not need to be calibrated, as it still ensures that wave breaking continues along the slope to the end of the domain.

In Fig. 6b, for the *B-RTFN* criterion, the crest celerity transitions from the LF method to the analytical approach shown in Eq.(6) in the interval $x \in [14.88, 15.47]\,m$ where wave breaking occurs. Compared to the experimental data (black points), the simulated crest celerity of the *B-RTFN* criterion and the B criterion is generally larger, though only

slightly. Notably, in the breaking region and its vicinity, the *B-RTFN* criterion aligns more closely with the experimental observations than the B criterion.

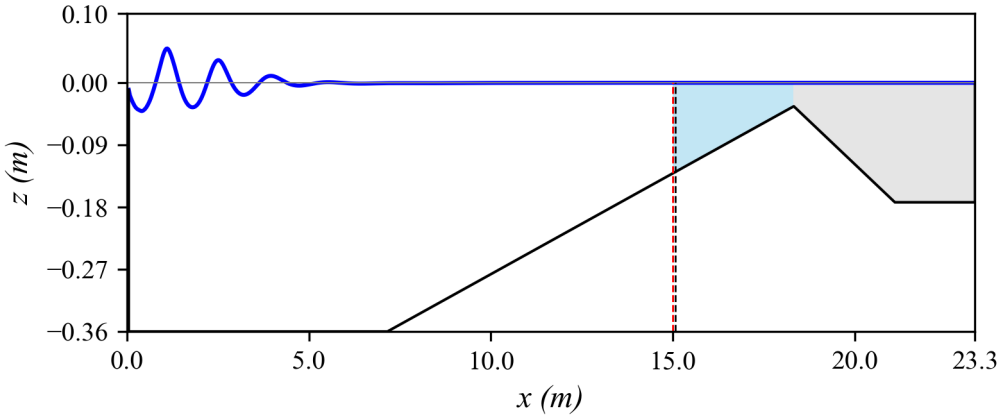

Figure 5: Bathymetry of Hansen and Svendsen (1979).

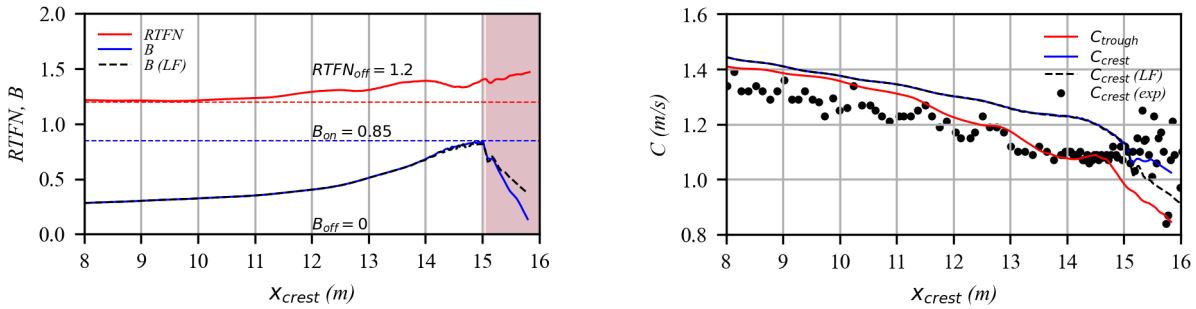

(a) Evolution of B and *RTFN*

(b) Evolution of the celerity

Figure 6: Breaking region in the case of Hansen and Svendsen (1979)

Next, we theoretically analyze this issue from the perspective of the definition of the *RTFN*. Knowing that the still water depth d is a function of x, and that the absorption region is not considered, the depth can be expressed as follows,

$$\begin{cases} d = d_0, & \text{if : } x \leq x_0 \\ d = m(x - x_0) + d_0, & \text{if : } x_0 < x \leq x_p \end{cases} \tag{7}$$

where d_0 represents the constant water depth, and x_0 denotes the position of the toe of the ramp, with a negative slope of m. The position of the wave crest is denoted as x_{crest}, while the corresponding trough is located at $x_{trough} = x_{crest} + \Delta x$, and Δx is the horizontal distance between the crest and the trough. Therefore, by combining Eq.(4) and Eq.(6), substituting in Eq.(7), and neglecting the particle velocity u_{trough} (since $u_{trough} \ll c_{crest}$), the *RTFN* can be transformed into:

$$RTFN = \frac{\sqrt{g(m(x_{crest} - x_0) + d_0)}}{\sqrt{g(m(x_{crest} + \Delta x - x_0) + d_0 + \eta)}} \tag{8}$$

Since the waveform changes gradually, it is assumed that both η and Δx are constant. Thus, it can be simplified into,

$$RTFN = \sqrt{\frac{mx_{crest} + a}{mx_{crest} + b}} \tag{9}$$

where both a and b are constants. Since both $m\Delta x$ and η are negative here, a is greater than b. It is easy to deduce that the *RTFN* is a monotonically increasing function, which explains why the *RTFN* increases rather than decreases when waves break over the slope.

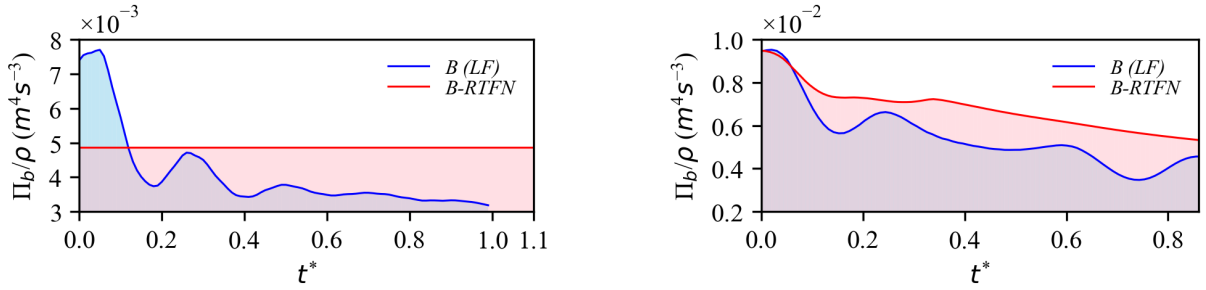

(a) Case BB (b) Case HS

Figure 7: Energy dissipation rate Π_b with respect to $t*$, the normalized time, where $t^* = \frac{t}{t_{off}-t_{on}}$; in the case of HS, wave breaking continues until the end of the domain, so t_{off} is defined as the the moment when the wave becomes too small to be detected.

Comparing the two criteria (see Fig. 8), there is almost no difference in the wave envelopes. The only distinction is that the wave crest in the simulation using the *B-RTFN* criterion decreases slightly faster, which is consistent with the BB case. The reason for this can also be seen in Fig. 7b: overall, the energy dissipation in the case of the *B-RTFN* criterion is greater than that of the *B* criterion.

During wave breaking, a distinction can be observed between the two types of wave breaking: spilling and plunging. In the case of spilling breaking, the deformation of the wave crest is gradual, and breaking does not occur at the peak of the wave height. As shown in Fig. 8, the elevation of the wave crest has already decreased to a certain extent by the time breaking begins. It is also validated by the experimental results, as shown in Fig. 9, where the breaking onset position ($x = 14.88\,m$) is represented by vertical dashed red line . In contrast, for plunging waves, there is a sharp change in the shape of the wave crests as they pass over the corner of the trapezoidal bar, resulting in breaking occurring almost at the peak of the wave height, as shown in Fig. 3.

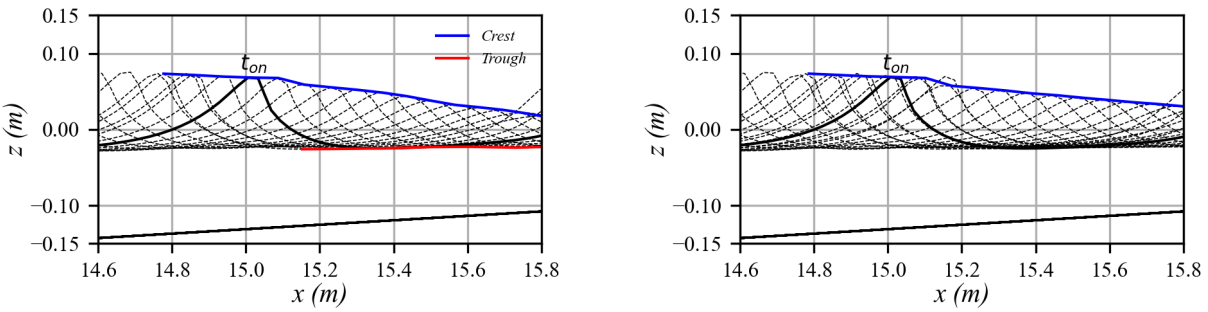

(a) using *B-RTFN* criterion (b) using *B* criterion

Figure 8: Envelope of the breaking wave, showing snapshots of the free surface position every 10 time steps, in the HS test case.

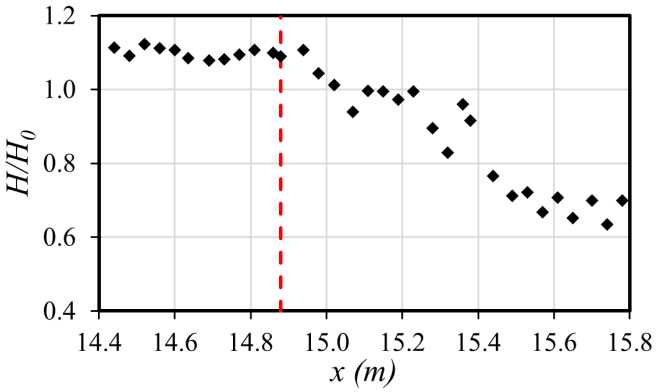

Figure 9: H/H_0 of the experimental results in the HS test case.

IV – Conclusion

The B criterion is generally regarded by some as a universal criterion for determining wave breaking onset. Overall, both experimental and numerical results have confirmed its accuracy with some exceptions, and the numerical simulations in this study also confirm this when comparing to two different experiments. However, this criterion has to be calibrated based on the water depth and specific bathymetry when using B to determine wave breaking termination.

By including the effect of the trough velocity c_{trough}, the $RTFN$ criterion addresses this issue to some extent. Since the elevation of the wave trough experiences less variation during wave propagation, the celerity at the trough provides a more objective measure of the downstream water depth than the B criterion. Combined with the wave celerity c_{crest} at the corresponding crest, the ratio of the two celerities can more accurately reflect the bathymetry changes between the location of the crest and trough, thereby providing a more precise assessment of the wave adaptation to the local bathymetry.

In conclusion, the $B - RTFN$ criterion enables a more universal identification of the breaking region, particularly improving the estimation of breaking termination, with $B_{on} = 0.85$ and $RTFN_{off} = 1.2$. However, to ensure the stability of numerical simulations, this study used the Ursell number to classify the wave nonlinearity when analyzing the B-$RTFN$ criterion, thereby simplifying the calculation of the wave celerity. While this approach enhances stability, it also limits the universality of this method to some extent, especially in deeper water conditions. When the shallow water assumption no longer holds, the accuracy of this method requires further investigation and analysis. It is important to note that the calculation of the celerity also influences the energy dissipation during wave breaking, which is especially evident in the BB case. Therefore, this issue will be a primary focus for analysis and resolution in future research.

Acknowledgments

The thesis work of J. Wang is supported by a scholarship from the China Scholarship Council (CSC) and the École nationale des ponts et chaussées.

References

[1] X. Barthelemy, M. Banner, W. Peirson, F. Fedele, M. Allis, and F. Dias. On a unified breaking onset threshold for gravity waves in deep and intermediate depth water. *Journal of Fluid Mechanics*, 841:463–488, 2018.

[2] S. Beji and J. Battjes. Experimental investigation of wave propagation over a bar. *Coastal Engineering*, 19(1-2):151–162, 1993.

[3] M. Derakhti, J. T. Kirby, M. L. Banner, S. T. Grilli, and J. Thomson. A unified breaking onset criterion for surface gravity water waves in arbitrary depth. *Journal of Geophysical Research: Oceans*, 125(7):e2019JC015886, 2020.

[4] S. T. Grilli and J. Horrillo. Numerical generation and absorption of fully nonlinear periodic waves. *Journal of engineering mechanics*, 123(10):1060–1069, 1997.

[5] S. T. Grilli, J. Horrillo, and S. Guignard. Fully nonlinear potential flow simulations of wave shoaling over slopes: Spilling breaker model and integral wave properties. *Water Waves*, 2(2):263–297, 2020.

[6] S. T. Grilli, J. Skourup, and I. Svendsen. An efficient boundary element method for nonlinear water waves. *Engng. Analysis with Boundary Elemts.*, 6(2):97–107, 1989.

[7] J. Hansen and I. Svendsen. Regular waves in shoaling water experimental data. Technical report, Institute of Hydrodynamics and Hydraulic Engineering, Technical University of Denmark, 1979.

[8] A. B. Kennedy, Q. Chen, J. T. Kirby, and R. A. Dalrymple. Boussinesq modeling of wave transformation, breaking, and runup. i: 1d. *Journal of waterway, port, coastal, and ocean engineering*, 126(1):39–47, 2000.

[9] S. Mohanlal, J. Harris, M. Yates, and S. Grilli. Unified depth-limited wave breaking detection and dissipation in fully nonlinear potential flow models. *Coastal Engineering*, 183:104316, 2023.

[10] T. Okamoto and D. R. Basco. The Relative Trough Froude Number for initiation of wave breaking: Theory, experiments and numerical model confirmation. *Coastal Engineering*, 53(8):675–690, 2006.

[11] T. Okamoto, C. J. Fortes, and D. R. Basco. Wave breaking termination on bar-trough shaped beaches. In *ISOPE International Ocean and Polar Engineering Conference*, pages ISOPE–I. ISOPE, 2008.

[12] H. A. Schäffer, P. A. Madsen, and R. Deigaard. A boussinesq model for waves breaking in shallow water. *Coastal engineering*, 20(3-4):185–202, 1993.

[13] Y.-M. Scolan and S. Etienne. Pressure analysis in nonlinear waves by revisiting the breaking wave onset. *European Journal of Mechanics-B/Fluids*, 101:246–256, 2023.

[14] B. Simon, C. E. Papoutsellis, M. Benoit, and M. L. Yates. Comparing methods of modeling depth-induced breaking of irregular waves with a fully nonlinear potential flow approach. *Journal of Ocean Engineering and Marine Energy*, 5(4):365–383, 2019.

[15] J.-B. Song and M. L. Banner. On determining the onset and strength of breaking for deep water waves. part i: Unforced irrotational wave groups. *Journal of Physical Oceanography*, 32(9):2541–2558, 2002.

[16] M. Utku. The relative trough froude number: a new wave breaking criteria. *unpublished Ph. D. dissertation, Civil Engineering Dept., Old Dominion University, Norfolk, Virginia*, 1999.